Neutron-scattering-based evidence for interacting magnetic excitons in LaCoO_{3}

S. El-Khatib, D. Phelan, J. G. Barker, H. Zheng, J. F. Mitchell, and C. Leighton

Phys. Rev. B **92**, 060404 — Published 6 August 2015

DOI: 10.1103/PhysRevB.92.060404

Revised version resubmitted to Phys. Rev. B. as a Rapid Communication on 7/23/2015

Neutron-scattering-based evidence for interacting magnetic excitons in $LaCoO_3$

S. El-Khatib[1,2,3], D. Phelan[2,4], J.G. Barker[3], H. Zheng[4], J.F. Mitchell[4] and C. Leighton[2]

[1]*Department of Physics, American University of Sharjah, PO Box 26666, Sharjah, United Arab Emirates*

[2]*Department of Chemical Engineering and Materials Science, University of Minnesota, Minneapolis, MN 55455, USA*

[3]*NIST Center for Neutron Research, National Institute of Standards and Technology, Gaithersburg, MD 20899, USA*

[4]*Materials Science Division, Argonne National Laboratory, Argonne, IL 60439, USA*

Recent progress with the thermally-driven spin-state crossover in $LaCoO_3$ has made it increasingly apparent that the nominally non-magnetic low spin ground state of this material actually hosts novel defect-based magnetism. This is investigated here *via* a small-angle neutron scattering (SANS) study of $LaCoO_{3-\delta}$ crystals. The results provide: (*i*) the surprising finding that the spin-state crossover is clearly reflected in SANS *via* quasielastic/inelastic scattering from paramagnetic spin fluctuations/excitations, and (*ii*) evidence for the formation, likely around oxygen defects, of local entities known as magnetic excitons. The latter generate distinct magnetic scattering below 60 K, providing valuable quantitative information on exciton densities and interactions. Potential relevance to the unexpected ferromagnetism recently discovered in epitaxial $LaCoO_3$ films is discussed.

PACS Nos: 75.47.Lx, 75.30.Wx, 75.25.-j

Corresponding author: CL (leighton@umn.edu)

Magnetism in $LaCoO_3$ has attracted attention and controversy for almost 50 years, largely due to the only marginal dominance of the crystal field splitting of t_{2g} and e_g states over the Hund exchange energy [1,2]. A low spin (LS, $t_{2g}^6 e_g^0$, $S = 0$) configuration is thus observed in the ground state, but is stable only to ~30 K, at which point excited spin-states are gradually populated [1-12]. These excited states can be simplistically described as intermediate spin (IS, $t_{2g}^5 e_g^1$, $S = 1$) and/or high spin (HS, $t_{2g}^4 e_g^2$, $S = 2$), but unravelling the true nature of the thermally-excited paramagnetism has proven a formidable challenge. Experimentally, mixed, and even contradictory conclusions have been obtained on the relative stability of IS and HS states [1-12], while theoretical difficulties also abound [13-17]. An example of the latter is that local analyses [1,15] and band structure approaches [13,16,17] often favor different excited states due to the differing extents to which they capture Co-O hybridization [14,17], spin-orbit interactions [15], *etc*.

Despite these challenges, substantial recent progress has been achieved. This encompasses: (*i*) Increased recognition that characterization of excited states as atomic-like "IS" or "HS" is likely misleading due to significant spin-orbit coupling [15] and Co-O covalency [17]; (*ii*) A suite of experiments using electron spin resonance [6,11], X-ray absorption spectroscopy/magnetic circular dichroism [7], and inelastic neutron spectroscopy (INS) [8,9], that consistently identify a zero-field-split triplet as the first excited state; (*iii*) Direct measurement of both a 0.6 meV excitation associated with this triplet [8,9] and a *g*-factor of 3-3.5 [6,11]; and (*iv*) Consistent interpretation of these results in terms of a spin-orbit triplet excited state [6,8,9,11,15]. While the understanding of the spin-state problem in $LaCoO_3$ thus remains incomplete, it is nevertheless advancing.

Remarkably, recent work has also emphasized that the challenges and controversies with magnetism in $LaCoO_3$ extend even to the nominally "non-magnetic" ($S = 0$) LS ground state. An unexpected transition to a weak FM state at temperatures between 50 and 100 K has in fact been detected by several groups [*e.g.*18-21], some form of defect-based magnetism being implicated. The possibility of surface FM has been discussed [18,20,21], as have local FM entities termed magnetic excitons [19]. The latter were predicted by Nagaev and Podel'shchikov [22], the essential concept being that doped carriers created at defects in $LaCoO_3$ (for instance electrons induced at oxygen vacancies) can stabilize finite spin Co ions within their localization volume. Specifically, analytical calculations [22] show the stability of magnetoexcitonic complexes where the total energy is lowered by trapping the electron, exciting HS Co ions inside the complex, and aligning their moments. Such a "magnetic exciton" is thus distinguished from a "magnetic polaron" by the *induction* of the moments in addition to their alignment. Low field magnetization and muon spin relaxation measurements support the existence of these excitons [19,23], as does retention of some finite spin Co even as $T \rightarrow 0$, as seen in specific heat [24]. Parallels with the "spin-state polarons" that form with dilute Sr (*i.e.* hole) doping [4,25] are obvious, potentially playing an important role [19,23,26] in seeding the nanoscale magnetic inhomogeneity in $La_{1-x}Sr_xCoO_3$ [27]. Noteworthy in comparison to conventional magnetic polarons is that these excitons / spin-state polarons form as the host lattice crosses over to an $S = 0$ ground state; they can thus exist in a non-magnetic (as opposed to para- or antiferro-magnetic) matrix.

Here, a study of the magnetism of $LaCoO_3$ crystals using small-angle neutron scattering (SANS) is reported. The magnetic SANS is found to have two contributions: A low scattering wavevector (q) part with strong q dependence that turns on below 60 K, and a higher q part with

negligible q dependence that increases gradually on warming above 30 K. The latter is shown to be due to the spin-state crossover, which SANS is demonstrated to be sensitive to *via* the quasielastic and low energy inelastic scattering from paramagnetic spin fluctuations and excitations. Most importantly, the low q scattering is found to be of Guinier type, revealing a bulk ensemble of scattering centers that are identified as magnetic excitons. The results provide information on the size, density, and interactions of these excitons, constituting a direct neutron-based observation of their existence. Potential relevance to the now well documented observation of unexpected FM in epitaxial thin films of $LaCoO_3$ is discussed.

The $LaCoO_3$ samples used in this study are from the series of floating-zone-grown $La_{1-x}Sr_xCoO_3$ single crystals extensively characterized and discussed in prior work [*e.g.* 8,11,12,24,27]. $LaCoO_{3-\delta}$ is a more accurate representation of their stoichiometry, the density of defect-stabilized $T \rightarrow 0$ finite spin Co ions from the 0.5 meV specific heat Schottky anomaly suggesting $\delta \approx 0.0005$ [24]. Zero-field-cooled magnetization (M) measurements were performed on these crystals in a superconducting quantum interference device magnetometer from 2-300 K in fields ($\mu_0 H$) from 0.05 to 5 T. SANS measurements were made between 5 and 300 K on the NG7 and NG3 instruments at the NIST Center for Neutron Research, at a wavelength, $\lambda = 5$ Å. The scattering was recorded on a 2D area detector, using circular averaging to obtain the absolute cross-section ($d\Sigma/d\Omega$) *vs*. the magnitude of the scattering wavevector, $|\vec{q}| = q$. The probed range ($0.014 \leq q \leq 0.240$ Å^{-1}) was obtained at a single sample-to-detector distance.

The q dependence of $d\Sigma/d\Omega$ is shown in Fig. 1 at four representative temperatures between 5 and 300 K. Two distinct q regimes are apparent: A low q regime ($q < 0.03$ Å^{-1}) where $d\Sigma/d\Omega$ is a steep function of q and increases quickly on cooling below ~60 K, and a high q regime ($q > 0.03$

Å^{-1}) where $d\Sigma/d\Omega$ is notably q-independent, increasing gradually on *warming* above ~30 K. The T dependence in these two q regimes can be seen more clearly in Fig. 2 (panels (b) through (e)), where it is compared to M/H (panel (a)). The latter readily illustrates the phenomena discussed in the introduction, the rising susceptibility on cooling below 300 K reflecting the Curie-Weiss behavior of excited Co ions, the falling susceptibility between 100 and 30 K marking the spin-state crossover, and the increase at the lowest T (particularly in low H) being due to the defect-based magnetism. Lower fields and more specialized field-cooling protocols [19,23] reveal the saturating component associated with the weak FM discussed above, as can be seen for instance in Figure 4 of ref. 19. As shown in Figs. 2(b,c), in the low q regime (< 0.03 Å^{-1}) $d\Sigma/d\Omega$ is essentially T-independent down to ~60 K, below which it increases monotonically by as much as 40 %. In the high q regime (> 0.03 Å^{-1}, Figs. 2(d,e)) the behavior is very different, the low T upturn progressively weakening with increasing q, accompanied by a clear increase in $d\Sigma/d\Omega(T)$ from 30 to 300 K. While the scattering at such q values is quite weak, making incoherent scattering a potential concern, simple estimates place this at only 20-30 % of even the minimum cross-section shown in Fig. 2(e). Moreover, this incoherent contribution is expected to be both q and T independent. Also worth emphasizing is that Figs. 2(b-e) plot $d\Sigma/d\Omega$ values computed from circular averages in the q_x-q_y plane. The scattering from these crystals has small, but non-zero anisotropy however, which can be quantified by the parameter $A = [(d\Sigma/d\Omega)_{max} - (d\Sigma/d\Omega)_{min}] / (d\Sigma/d\Omega)_{min} \times 100$ %, where "max" and "min" denote the maximum and minimum values on a circular scan at fixed q. Fig. 2(f) shows $A(T)$ at a representative q of 0.08 Å^{-1}, the striking feature being the similarity to both $d\Sigma/d\Omega(T)$ at similar q (Fig. 2(e)) and $M/H(T)$ (Fig. 2(a)).

There are two main (*T*-dependent) features of interest that emerge from Figs. 1 and 2: The gradual increase in the *q*-independent scattering on warming from 30 to 300 K for $q > 0.03$ Å^{-1} (*e.g*. Figs. 2(d,e)), and the more abrupt increase in the strongly *q*-dependent scattering on cooling below 60 K for $q < 0.03$ Å^{-1} (*e.g*. Figs. 2(b,c)). The origin of these two features is now discussed in turn. Given the *q* independence (which implies a local origin), the onset temperature (30 K), and the monotonic increase in $d\Sigma/d\Omega$ on warming, the obvious question with the scattering at $q > 0.03$ Å^{-1} (Figs. 2(d,e)) is whether it could somehow reflect the spin-state crossover. The inelastic neutron spectroscopy (INS) data of Phelan *et al* [8] are important in this context, having demonstrated that warming $LaCoO_3$ above 30 K induces both a broad inelastic continuum centered at energy transfer, $\Delta E = \hbar\omega = 0$, as well as well-defined excitations at ± 0.6 meV. The former derives from paramagnetic spin fluctuations, the latter the 0.6 meV excitation of the excited state triplet discussed above. The dynamic structure factor from such data, $S(\vec{q},\omega)$, is related to the imaginary part of the dynamic magnetic susceptibility by $S(\vec{q},\omega) = \frac{\chi''(\vec{q},\omega)}{1-e^{\frac{-\hbar\omega}{kT}}}$, and $\chi''(\omega)$ from 0.5 – 2.0 Å^{-1} was found to be well described by:

$$\chi''(\omega) = \frac{\chi_0\Gamma_0\hbar\omega}{(\hbar\omega)^2+\Gamma_0^2} + \frac{\chi_1\Gamma_1\hbar\omega}{(\hbar\omega+\hbar\omega_0)^2+\Gamma_1^2} + \frac{\chi_1\Gamma_1\hbar\omega}{(\hbar\omega-\hbar\omega_0)^2+\Gamma_1^2} \qquad (1).$$

Here χ_0 is the static susceptibility, χ_1 is the susceptibility associated with the 0.6 meV excitation, Γ_0 and Γ_1 are relaxation rates, and $\hbar\omega_0$ = 0.6 meV. The first term captures the inelastic continuum, the second and third the ± 0.6 meV excitations. Phelan *et al* thereby determined χ_0, χ_1, Γ_0, and Γ_1 as a function of *T*, which were found to clearly reflect the spin-state crossover [8].

To connect to the current work it is first important to acknowledge that in SANS, λ is held approximately constant, $d\Sigma/d\Omega$ is measured *vs*. the scattering angle 2θ, and elastic scattering is

typically assumed, leading to $q=|\vec{q}|=(4\pi \sin\theta)/\lambda$. However, the quasielastic and low energy inelastic processes captured by equation 1 may also contribute to the SANS cross-section. $|\vec{q}|$ should then be more generally written as:

$$|\vec{q}|^2=\left|\vec{k}_i\right|^2+\left|\vec{k}_f\right|^2-2\left|\vec{k}_i\right|\left|\vec{k}_f\right|\cos(2\theta) \qquad (2).$$

Here $\hbar\omega = E_i - E_f$, and E_i and E_f are the initial and final neutron kinetic energies given by $\frac{|\hbar\vec{k}_i|^2}{2m}$ and $\frac{|\hbar\vec{k}_f|^2}{2m}$, where m is the neutron mass. The scattering at fixed 2θ thus probes the integral of some trajectory through $\hbar\omega$-$|\vec{q}|$ space such that:

$$\frac{d\Sigma}{d\Omega}(2\theta) \propto \int_{-\infty}^{E_i} \frac{|\vec{k}_f|}{|\vec{k}_i|} f(\vec{q})^2 S(\vec{q},\omega) d\omega \qquad (3),$$

where $f(\vec{q})$ is the form factor. For magnetic scattering this gives:

$$\frac{d\Sigma}{d\Omega}(2\theta) \propto \int_{-\infty}^{E_i} \frac{|\vec{k}_f|}{|\vec{k}_i|} f(\vec{q})^2 \frac{\chi''(\vec{q},\omega)}{1-e^{\frac{-\hbar\omega}{kT}}} d\omega \qquad (4),$$

which, in conjunction with equation 1 and $\chi_0(T)$, $\chi_1(T)$, $\Gamma_0(T)$, $\Gamma_1(T)$ from Phelan *et al* [8], can be used to predict $d\Sigma/d\Omega(T)$ at the elastic q-values probed in the current SANS measurements. The results are indicated by the small red points in Figs. 2(d,e) (right axis), the excellent overall agreement with the data providing strong evidence that the increase in the q-independent SANS cross-section on warming above 30 K for q > 0.03 Å is indeed magnetic in origin, deriving from the thermal spin-state crossover. Comparing $A(T)$ (Fig. 2(f)), $d\Sigma/d\Omega(T)$ (Fig. 2(e)), and $M/H(T)$ (Fig. 2(a)) this magnetic scattering is apparently anisotropic. Note that while phonons may also contribute in Figs. 2(d,e), calculations based on ref. 28 and literature data for $LaCoO_3$ indicate a qualitatively different form than the measured T dependence, particularly below ~100 K.

Turning now to the strongly q-dependent SANS in the lower q region (< 0.03 Å^{-1}, Fig. 1), the first point to emphasize is the abrupt increase in $d\Sigma/d\Omega$ below 60 K (Figs. 2(b,c)), some form of magnetic scattering being one possible source. The onset temperature is in fact strikingly similar to the weak FM transition seen in the magnetometry and muon spin relaxation studies discussed above [19,23]. To further investigate this, the 300 K cross-section was subtracted from the data of Fig.1 generating the $d\Sigma/d\Omega(q)$ shown in the inset. Significantly, this is well described (solid line fits) by the Guinier form characteristic of the low q limit of a dilute assembly of scattering centers, *i.e.* $d\Sigma/d\Omega = (d\Sigma/d\Omega)_0 \exp(-q^2R_g^2)$, where $(d\Sigma/d\Omega)_0$ is the $q = 0$ Guinier cross-section, and R_g is the radius of gyration of the scatterers. The resulting $(d\Sigma/d\Omega)_0(T)$ and $R_g(T)$ are shown in Figs. 3(a,b). $(d\Sigma/d\Omega)_0$ is found to turn on quite sharply below 60 K (Fig. 3(a)), the corresponding R_g *decreasing* on cooling, from ~170 Å at the first point of detection, to 140 Å at low T (Fig. 3(b)) [29]. The latter observation is significant, as this is exactly the behavior of magnetic polarons in classic magnetic semiconductors such as $Cd_{1-x}Mn_xTe$ and $Cd_{1-x}Mn_xSe$, where the increase in polaron binding energy on cooling drives a decrease in radius [30-32]. Given this characteristic behavior of $R_g(T)$ (Fig. 3(b)), the q dependence expected of a bulk ensemble of local scattering centers (Fig. 1, inset), and the onset at the 60 K seen in prior work (Fig. 3(a)) [19,23], it is concluded that this scattering indeed derives from magnetic excitons. Any potential higher q features due to $f(q)$ and/or $S(q)$ are apparently obscured by background and other scattering contributions. Note that the observations presented here, particularly the Guinier q dependence, are consistent with magnetism throughout the bulk of the material.

One surprising aspect of Fig. 3 is the overall magnitude of the extracted R_g values. The 140 Å found at low T, for example, corresponds to ~35 pseudocubic unit cells, significantly exceeding the few lattice constants expected from theory [22], simple estimates from experimental data [4],

and measurements of analogous spin-state polarons in lightly hole-doped $LaCoO_3$ [25]. Analysis of the absolute magnitude of $(d\Sigma/d\Omega)_0$ sheds light on this issue. From elementary theory [33], $(d\Sigma/d\Omega)_0 = nV^2\langle(\Delta\rho)^2\rangle$, where n, V, and $\Delta\rho$ are the density, volume, and contrast of the scattering centers. Assuming this contrast is magnetic leads to $(d\Sigma/d\Omega)_0 \approx nC^2M^2$, where $C = 2.6 \times 10^{-5}$ $\text{Å}\mu_B^{-1}$, and M is the exciton magnetization in μ_B [34]. The low T experimental value of $(d\Sigma/d\Omega)_0 \approx 1$ cm^{-1} (Fig. 3(a)) thus constrains the product nC^2M^2, generating the n-M relation shown in Fig. 3(c), inspection of which immediately reveals that it is highly unlikely that the observed scattering is from an ensemble of isolated, non-interacting excitons. For example, assuming a typical individual exciton magnetization of ~20 μ_B results from this plot in an unphysical n of more than 10^{22} cm^{-3} (red dashed lines in Fig. 3(c)); in essence the observed scattering is too strong to result from entities with $M \sim 20$ μ_B. An alternative approach is to take the previously determined density of $T \rightarrow 0$ finite-spin Co ions (0.1 % of the sites, 2×10^{19} cm^{-3} [24]), assume these to reside in HS excitons, and use this to constrain n and M in conjunction with Fig. 3(c). The result of such a calculation is $n \sim 10^{14}$ cm^{-3}, $M \sim 5 \times 10^5$ μ_B (green dashed lines in Fig. 3(c)), *i.e.* a much lower density of higher M objects. Remarkably, this M is very close to that expected from an HS object with $R_g = 140$ Å (Fig. 3(b)), *i.e.* it is consistent with $d\Sigma/d\Omega(q)$. The clear implication is that the scattering observed here results not from isolated individual magnetic excitons, but rather interacting statistical agglomerates of such excitons with large M. Importantly, this is in accord with a true phase transition to a weak (low volume fraction) FM state, consistent with both Fig. 3(a) and prior ideas [19,23].

In summary, SANS measurements on single crystal $LaCoO_3$ have been shown to be sensitive both to the thermally driven spin-state crossover (*via* quasielastic/inelastic scattering from spin

fluctuations/excitations) and the formation of magnetic excitons in the ground state. The latter are evidenced by the onset of a Guinier scattering contribution below 60 K, analysis of which points to statistical agglomerates of interacting excitons. As a final comment on the implications of these findings, it is noted that recent years have seen a flurry of interest in heteroepitaxial thin films of $LaCoO_3$ due to the discovery of unexpected FM (or ferrimagnetism) [35]. While the majority of work has focused on strain-induced changes in electronic structure as an explanation, results such as those presented here indicate that an important role for oxygen vacancies should not be discounted. Very recent studies in fact implicate oxygen vacancy ordering as essential for the magnetic ordering [36]; the interplay between such defect ordering and magnetic exciton formation in $LaCoO_3$ is thus a fascinating topic for further study.

Acknowledgments: Work supported primarily by the US DOE under DE-FG02-06ER46275. Work at ANL (crystal growth and characterization) supported by DOE Office of Science, Basic Energy Sciences, Materials Science and Engineering Division. Part of this work was carried out in the UMN Characterization Facility, which receives capital equipment funding from the NSF through the UMN MRSEC under DMR-1420013. S.E-K. acknowledges travel support from AUS (FRG-2012, FRG2013). We thank F.S. Bates for useful discussions, and J.A. Borchers for experimental assistance.

References

[1] P.M. Raccah and J.B. Goodenough, Phys. Rev. **155**, 932 (1967).

[2] For a short review see p. 1235-1239 of M. Imada, A. Fujimori and Y. Tokura, Rev. Mod. Phys. **70**, 1039 (1998).

[3] K. Asai, O. Yokokura, N. Nishimori, H. Chou, J.M. Tranquada, G. Shirane, S. Higuchi, Y. Okajima and K. Kohn, Phys. Rev. B. **50**, 3025 (1994).

[4] S. Yamaguchi, Y. Okimoto, H. Taniguchi and Y. Tokura, Phys. Rev. B. **53**, R2926 (1996)

[5] P.G. Radaelli and S.W. Cheong, Phys. Rev. B. **66**, 094408 (2002).

[6] S. Noguchi, S. Kawamata, K. Okuda, H. Nojiri and M. Motokawa, Phys. Rev. B. **66**, 094404 (2002).

[7] M.W. Haverkort, Z. Hu, J.C. Cezar, T. Burnus, H. Hartmann, M. Reuther, C. Zobel, T. Lorenz, A. Tanaka, N.B. Brookes, H.H. Hsoeh, H.-J. Lin, C.T. Chen and L.H. Tjeng, Phys. Rev. Lett. **97**, 176405 (2006).

[8] D. Phelan, D. Louca, S. Rosenkranz, S.-H. Lee, Y. Qui, P.J. Chupas, R. Osborn, H. Zheng, J.F. Mitchell, J.R.D. Copley, J.L. Sarrao and Y. Moritomo, Phys. Rev. Lett. **96**, 027201 (2006).

[9] A. Podlesnyak, S. Streule, J. Mesot, M. Medarde, E. Pomjakushina, K. Conder, A. Tanaka, M.W. Haverkort and D.I. Khomskii, Phys. Rev. Lett. **97**, 247208 (2006).

[10] D.P. Kozlenko, N.O. Golosova, Z. Jirak, L.S. Dubrovinsky, B.N. Savenko, M.G. Tucker, Y.L. Godec and V.P. Glazkov, Phys. Rev. B. **75**, 064422 (2007).

[11] M.J.R. Hoch, S. Nellutla, J. van Tol, E.S. Choi, J. Lu, H. Zheng and J.F. Mitchell, Phys. Rev. B. **79**, 214421 (2009).

[12] N. Sundaram, Y. Jiang, I.E. Anderson, D.P. Belanger, C.H. Booth, F. Bridges, J.F. Mitchell, T. Proffen and H. Zheng, Phys. Rev. Lett. **102**, 026401 (2009).

[13] M.A. Korotin, S. Yu. Ezhov, I.V. Solovyey, V.I. Anisimov, D.I. Khomskii and G.A. Sawatzky, Phys. Rev. B. **54**, 5309 (1996).

[14] K. Tsutsui, J. Inoue and S. Maekawa, Phys. Rev. B. **59**, 4549 (1999)

[15] Z. Ropka and R.J. Radwanski, Phys. Rev. B. **67,** 172401 (2003).

[16] H. Hsu, P. Blaha, R.M. Wentvcovitch and C. Leighton, Phys. Rev. B. **82**, 100406(R) (2010).

[17] Y. Lee and B.N. Harmon, J. Appl. Phys. **113**, 17E145 (2013).

[18] J.-Q. Yan, J.-S. Zhou and J.B. Goodenough, Phys. Rev. B. **70**, 014402 (2004).

[19] S.R. Giblin, I. Terry, S. Clarke, T. Prokscha, A.T. Boothroyd, J. Wu and C. Leighton, Europhys. Lett. **70**, 677 (2005).

[20] A. Harada, T. Taniyama, Y. Takeuchi, T. Sato, T. Kyomen and M. Itoh, Phys. Rev. B. **75**, 184426 (2007).

[21] A.M. Durand, D.P. Belanger, C.H. Booth, F. Ye, S. Chi, J.A. Fernandez-Baca and M. Bhat, J. Phys.: Cond. Mat. **25**, 382203 (2013).

[22] E.L. Nagaev and A.I. Podelshchikov, J. Phys.: Cond. Mat. **8**, 5611 (1996).

[23] S.R. Giblin, I. Terry, D. Prabhakaran, A.T. Boothroyd, J. Wu and C. Leighton, Phys. Rev. B. **74**, 104411 (2006).

[24] C. He, H. Zheng, J.F. Mitchell, M.L. Foo, R.J. Cava and C. Leighton, Appl. Phys. Lett., **94**, 102514 (2009).

[25] A. Podlesnyak, M. Russina, A. Furrer, A. Alfonsov, E. Vavilova, V. Kataev, B. Buchner, Th. Strassle, E. Ponjakushina, K. Conder and D.I. Khomskii, Phys. Rev. Lett. **101**, 247603 (2008).

[26] A. Podlesnyak, G. Ehlers, M. Frontzek, A.S. Sefat, A. Furrer, Th. Strässle, E. Pomjakushina, K. Conder, F. Demmel, and D.I. Khomskii, Phys. Rev. B. **83**, 134430 (2011).

[27] See for example C. He, S. El-Khatib, J. Wu, J.W. Lynn, H. Zheng, J.F. Mitchell and C. Leighton, Europhys. Lett. **87**, 27006 (2009).

[28] J.G. Barker and D.F.R. Mildner, in press, J. Appl. Cryst. (2015).

[29] Based on these values of R_g (Fig. 3(b)) the validity of the Guinier form would be expected to be restricted to $q < 0.01$ Å^{-1}, whereas it actually extends to at least 0.03 Å^{-1} (Fig. 1, inset). This applicability beyond the range rigorously expected is not uncommon however; see for example J.S. Higgins and H.C. Benoit, *Polymers and Neutron Scattering*, Oxford, 1994.

[30] T. Dietl, in *Handbook on Semiconductors*, vol. 3, pp 1291, ed. T.S. Moss, Elsevier (1994).

[31] M. Sawicki, T. Dietl, J. Kossut, J. Igalson, T. Wojtowicz and W. Plesiewicz, Phys. Rev. Lett. **56**, 508 (1986).

[32] C. Leighton, I. Terry and P. Becla, Phys. Rev. B. **58**, 9773 (1998).

[33] A. Furrer, J. Mesot and T. Strassle, *Neutron Scattering in Condensed Matter Physics*, World Scientific (2009).

[34] This step requires information on the angle between $\vec{q}$ and the magnetization vector. Assuming randomly oriented magnetization leads to $(d\Sigma/d\Omega)_0 = (1/2)nC^2M^2$. Here we simply approximate $(d\Sigma/d\Omega)_0 \approx nC^2M^2$.

[35] D. Fuchs, C. Pinta, T. Schwarz, P. Schweiss, P. Nagel, S. Schuppler, R. Schneider, M. Merz, G. Roth and H. von Lohneysen, Phys. Rev. B. **75**, 144402 (2007).

[36] N. Biskup, J. Salafranca, V. Mehta, M.P. Oxley, Y. Suzuki, S.J. Pennycook, S.T. Pantiledes and M. Varela, Phys. Rev. Lett. **112**, 087202 (2014).

Figure Captions

Figure 1: Wavevector (q) dependence of the scattering cross-section ($d\Sigma/d\Omega$) at representative temperatures of 5, 40, 80 and 300 K. Inset: q dependence of the 300 K background subtracted cross-section at 5, 15, 30, 40, 80 and 100 K. The solid lines are fits to the Guinier form, as discussed in the text.

Figure 2: Temperature (T) dependence of: (a) M/H (M = magnetization, H = applied magnetic field) at H = 0.05 and 5 T, (b) $d\Sigma/d\Omega$ at q = 0.014 Å^{-1}, (c) $d\Sigma/d\Omega$ at q = 0.024 Å^{-1}, (d) $d\Sigma/d\Omega$ at q = 0.05 Å^{-1}, (e) $d\Sigma/d\Omega$ at q = 0.1 Å^{-1}, and (f) A at q = 0.08 Å^{-1}. The parameter A is defined as $[(d\Sigma/d\Omega)_{max} - (d\Sigma/d\Omega)_{min}] / (d\Sigma/d\Omega)_{min} \times 100$ %, where "max" and "min" denote the maximum and minimum values on a 360 ° angular scan at fixed q. All dashed lines are spline fits to guide the eye. On (d) and (e) the red points (right axis) denote $d\Sigma/d\Omega$ calculated from published inelastic neutron spectroscopy (INS) data, as discussed in the text.

Figure 3: T dependence of (a) the Guinier cross-section, $(d\Sigma/d\Omega)_0$ and (b) the radius of gyration, R_g, as determined from the fits in the inset to Fig. 1. The dashed lines are guides to the eye. In (a) the 100 K value was subtracted as a background. (c) Exciton density (n) – exciton magnetization (M) relation, determined by $(d\Sigma/d\Omega)_0 \approx nC^2M^2$, where $(d\Sigma/d\Omega)_0$ is fixed at its low temperature value from (a) (1.0 cm^{-1}).

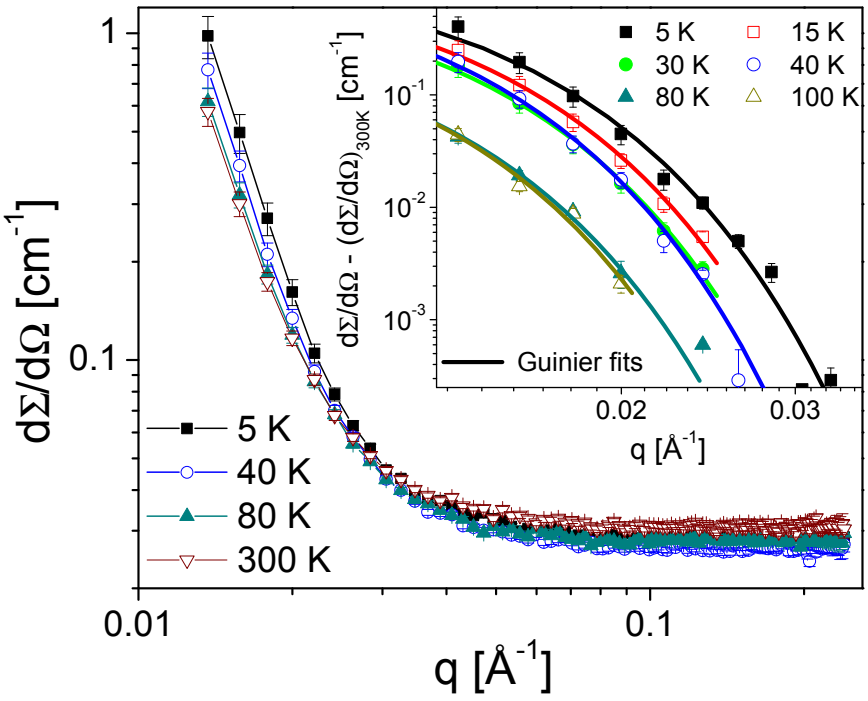
1
0.1
0.01
0.1
dΣ/dΩ [cm-1]
q [Å-1]
5 K
40 K
80 K
300 K
dΣ/dΩ - (dΣ/dΩ)300K [cm-1]
10-1
10-2
10-3
5 K
15 K
30 K
40 K
80 K
100 K
Guinier fits
0.02
0.03
q [Å-1]

Figure 1

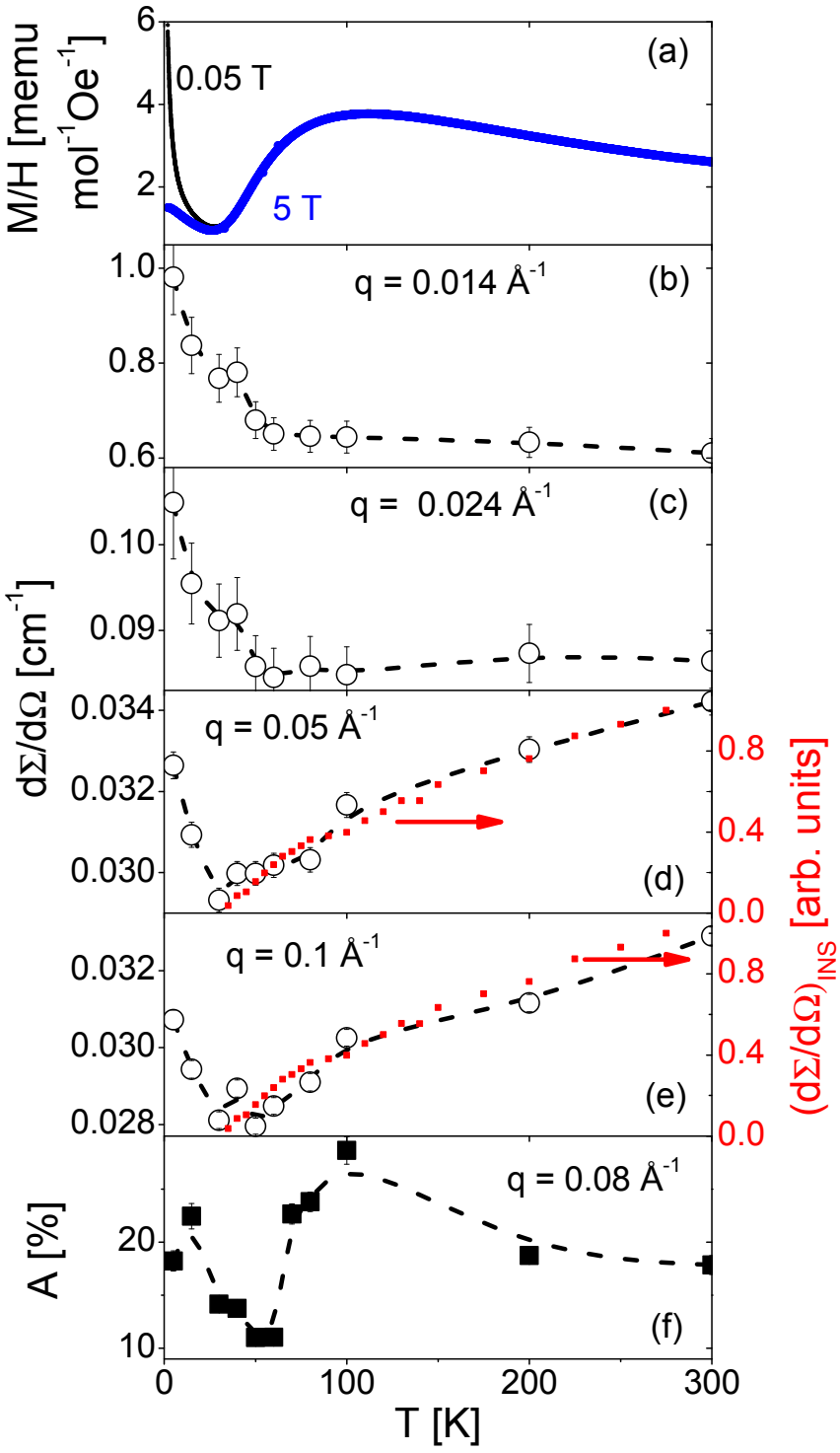
M/H [memu mol^{-1}Oe^{-1}]
0.05 T
5 T
(a)
q = 0.014 Å^{-1}
(b)
q = 0.024 Å^{-1}
(c)
dΣ/dΩ [cm^{-1}]
q = 0.05 Å^{-1}
(d)
q = 0.1 Å^{-1}
(e)
(dΣ/dΩ)$_{INS}$ [arb. units]
A [%]
q = 0.08 Å^{-1}
(f)
T [K]

Figure 2

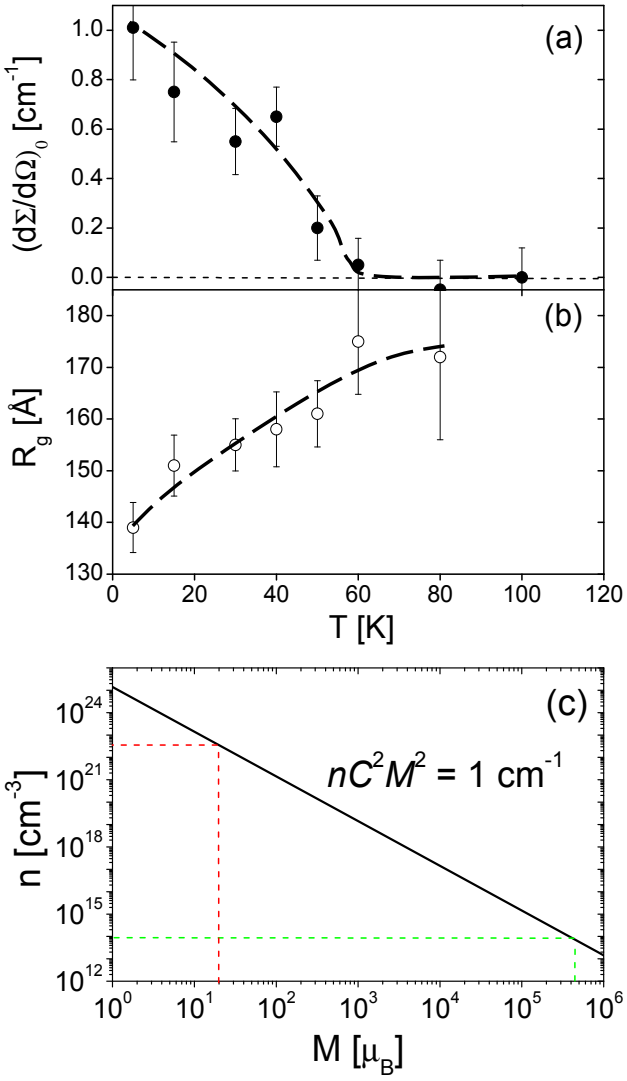

Figure 3